

circ-0000512 inhibits PD-L1 ubiquitination through sponging miR-622/CMTM6 axis to promote triple-negative breast cancer and immune escape

Li-Feng Dong ¹, Fang-Fang Chen,² Yang-Fan Fan,² Kun Zhang,¹ Hui-Hui Chen¹

To cite: Dong L-F, Chen F-F, Fan Y-F, *et al.* circ-0000512 inhibits PD-L1 ubiquitination through sponging miR-622/CMTM6 axis to promote triple-negative breast cancer and immune escape. *Journal for ImmunoTherapy of Cancer* 2023;11:e005461. doi:10.1136/jitc-2022-005461

► Additional supplemental material is published online only. To view, please visit the journal online (<http://dx.doi.org/10.1136/jitc-2022-005461>).

Accepted 31 May 2023



© Author(s) (or their employer(s)) 2023. Re-use permitted under CC BY-NC. No commercial re-use. See rights and permissions. Published by BMJ.

¹Department of Breast Surgery and Oncology, Key Laboratory of Cancer Prevention and Intervention, Ministry of Education, The Second Affiliated Hospital, Zhejiang University School of Medicine, Hangzhou, Zhejiang, People's Republic of China

²Department of Breast Surgery, Women's Hospital, Zhejiang University School of Medicine, Hangzhou, Zhejiang, People's Republic of China

Correspondence to

Dr Li-Feng Dong;
lifengdong@zju.edu.cn

ABSTRACT

Background This study reported the function and mechanism of circ-0000512 in the progression of triple-negative breast cancer (TNBC).

Methods circ-0000512 expression in TNBC tissues and paired adjacent normal tissues and cells was examined by qRT-PCR. Moreover, circ-0000512 expression in TNBC cells was modulated by transfection. Thereafter, colony formation assay, Transwell assay and flow cytometry were conducted to observe cell proliferation, migration and apoptosis. TNBC cells were treated with cycloheximide and the protease inhibitor MG132. Later, ubiquitination assay was performed to detect programmed cell death ligand 1 (PD-L1) ubiquitination in TNBC cells. The T cell killing ability was assessed by the T cell-mediated tumor cell killing assay. IFN γ and IL-2 levels were detected by ELISA. The percentage of activated T cells was detected with a flow cytometer. In addition, dual luciferase reporter gene assay and RNA immunoprecipitation assay were carried out to evaluate the binding between two genes. In vivo study was conducted on mice. CD8⁺ T cells in xenograft tumors were detected by immunohistochemistry.

Results circ-0000512 was upregulated in patients with TNBC. circ-0000512 knockdown attenuated the proliferation and migration of TNBC cells and enhanced their apoptosis. circ-0000512 overexpression had opposite effects. circ-0000512 knockdown enhanced the PD-L1 protein ubiquitination in TNBC cells by inhibiting CMTM6. Meanwhile, circ-0000512 promoted CMTM6 expression by sponging miR-622. circ-0000512 knockdown increased the ratio of CD8⁺ T cells and the lethality of T cells against TNBC cells. Besides, circ-0000512 knockdown inhibited the growth of TNBC cells in immunodeficient nude mice and normal immune mice and increased the ratio of CD8⁺ T cells in xenograft tumors of normal immune mice.

Conclusions circ-0000512 inhibited PD-L1 ubiquitination by sponging the miR-622/CMTM6 axis, thus promoting TNBC progression and immune escape.

BACKGROUND

Triple-negative breast cancer (TNBC) is a subtype of breast cancer (BC), which lacks the expression of estrogen receptor, progesterone receptor and HER2.¹ TNBC accounts

WHAT IS ALREADY KNOWN ON THIS TOPIC

⇒ circ-0000512 has been identified to be an oncogene in colorectal cancer and is considered a promising target for the treatment of colorectal cancer. However, the function of circ-0000512 in triple-negative breast cancer (TNBC) has not yet been investigated.

WHAT THIS STUDY ADDS

⇒ This study first elucidated the function of circ-0000512 in TNBC, aiming to find a novel target for TNBC treatment.

HOW THIS STUDY MIGHT AFFECT RESEARCH, PRACTICE OR POLICY

⇒ circ-0000512 is an oncogene in TNBC, which may be an effective treatment target for TNBC clinically.

for about 24% of all the newly diagnosed BC cases.² Compared with other subtypes of BC, TNBC is characterized by its higher aggressiveness and susceptibility to early recurrence.³ It has been reported that the distant metastasis rate in patients with TNBC is about 46%.⁴ Even worse, the mortality rate of TNBC is as high as 40% within the first 5 years after diagnosis and about 75% within 3 months after recurrence.⁴ Although great progresses have been made in TNBC treatment, the recurrence rate, metastasis rate and drug resistance are still the main causes of death in patients with TNBC.⁵ Therefore, the precise pathogenesis of TNBC should be further verified to identify the more effective molecular target for treatment.⁶

Circular RNAs (circRNAs) are a class of non-coding RNAs with covalently closed-loop structures. Due to the absence of 5'-end or 3'-end, circRNAs cannot be degraded by RNA exonuclease and thus can be stably expressed in cells.⁷ Accumulating evidence

has demonstrated that circRNAs are widely expressed in cells and involved in BC progression.^{8,9} In our preliminary research, five upregulated circRNAs (including circ-0000520, circ-0000518, circ-0000514, circ-0000511 and circ-0000512) and five downregulated circRNAs (namely, circ-103345, circ-104270, circ-102051, circ-102619 and circ-102049) were identified in TNBC according to Gene expression omnibus (GEO)-based analysis. This study focused on the upregulated circRNAs. Among the five upregulated circRNAs, the expression levels of circ-0000518 and circ-0000512 were higher than those of the other three circRNAs. The function of circ-0000518 in BC has been studied previously.¹⁰ Therefore, this study aimed to investigate the function of circ-0000512 in TNBC.

circ-0000512 (also known as circ-000166) has been reported in previous research to be highly expressed in colorectal cancer (CRC) tissues.¹¹ Wang *et al.*¹² demonstrated that the high expression of circ_0000512 indicated poor survival of patients with CRC. Besides, circ_0000512 knockdown inhibited the colony formation and viability of CRC cells and accelerated their apoptosis. Similarly, Zhao *et al.*¹³ identified that circ_0000512 expression increased in colon cancer. Through the knockdown of circ_0000512, the malignant phenotypes (such as viability, colony formation, migration and invasion) and *in vivo* growth of colon cancer cells were significantly reduced. However, the function of circ-0000512 in TNBC has not yet been investigated. Thus, this article aimed to detect the expression of circ-0000512 in TNBC and explore its function.

Generally, circRNAs play roles of the competitive endogenous RNAs (ceRNAs, microRNA (miRNA) sponges) to regulate the expression of downstream target genes, thereby affecting the tumor cell phenotype.¹⁴ MiRNAs, a family of small non-coding RNAs with the length of 19–24 nucleotides, can regulate the expression of their target genes by suppressing mRNA translation or promoting mRNA degradation.^{15,16} As for miR-622, it has been discovered that the decreased miR-622 expression in BC cells facilitates the cell viability and migration capacities.¹⁷ It is found based on Circular RNA Interactome that, miR-622 interacts with circ_0000512. Simultaneously, CMTM6 is predicted to be a target of miR-622 via miRDB. In a previous study, CMTM6 is overexpressed in TNBC, which is associated with the poor progression-free survival (PFS) of patients.¹⁸ According to these findings, this study verified whether circ_0000512 regulated TNBC development by targeting the miR-622/CMTM6 axis. Findings in this research will provide an effective molecular target for TNBC treatment.

METHODS

GEO analysis

The dataset of GSE101123 was downloaded from GEO database. The differentially expressed circRNAs between tumor tissues and adjacent normal tissues from four TNBC cases were analyzed by heat map and volcano plots.

Patients and clinical samples

Patients with TNBC (n=15) diagnosed in Women's Hospital, Zhejiang University School of Medicine from September 2018 to November 2019 were enrolled in this study. All patients participated in this study voluntarily and signed the written informed consent.

The patient inclusion criteria were as follows: patients who voluntarily participated in the study; patients who were diagnosed with TNBC for the first time; patients who underwent surgical resection; patients with no previous treatment history of cancer-related diseases and patients with no other severe diseases. The patient exclusion criteria were shown below: patients who did not voluntarily take part in the study; patients who previously received cancer-related treatments and patients with other severe diseases. The tumor tissues and matched adjacent normal tissues harvested during surgery were immediately stored in a refrigerator at -80°C .

Cell lines and culture

The human breast epithelial cell line (MCF10A) and TNBC cell lines (Hs578T, MDA MB 231, MDA MB 436, MDA MB 468, BT549 and HCC1937) were purchased from the Shanghai Institute of Cell Biology (Shanghai, China). Cells were grown in Dulbecco's modification of eagle's medium (DMEM) supplemented with 10% fetal bovine serum (FBS, Solarbio, Beijing, China), 100 U/mL penicillin (Solarbio) and 100 $\mu\text{g}/\text{mL}$ streptomycin (Solarbio) under 37°C and 5% CO_2 conditions in a humidified incubator.

Plasmids and transfection

MDA MB 231 and Hs578T cells were transfected with Lipofectamine 3000 (Thermo Fisher Scientific, Waltham, MA, USA) in strict accordance with the manufacturer's instructions. shRNA targeting circ-0000512 in the 3'UTR region (#1: 5'-GGTGAGGTGAGTTCCCAGAGA-3' and #2: AGGTGAGGTGAGTTCCCAGAG) and the corresponding negative control (NC), circ-0000512-expression vectors and the corresponding empty vectors, shRNA targeting CMTM6 in the 3'UTR region (5'-TGGAGAACGGAGCGGTGTACA-3') and the corresponding NC, CMTM6-expression vectors and the corresponding empty vectors, miR-622 mimics and the corresponding mimics NC were all provided by Genechem (Shanghai, China). After transfection, MDA MB 231 and Hs578T cells were cultured in DMEM containing 10% FBS for 48 hours. The transfection efficiency was determined by quantitative reverse transcription PCR (qRT-PCR) or Western blotting (WB) assay.

Colony formation assay

MDA MB 231 and Hs578T cells were harvested and prepared as single-cell suspension (cell density, 2000 cells/mL) with DMEM (10% FBS). Then, 1 mL suspension was seeded into each well of the 6-well plates. Thereafter, cells were cultured for 14 days under 37°C and 5% CO_2 conditions. DMEM that contained 10% FBS was changed every

3 days. After 14 days, the remaining liquid in each well was discarded. Afterwards, cells attaching to the bottom were fixed with 4% paraformaldehyde for 15 min and stained with 0.1% crystal violet for 15 min. The number of colonies formed (more than 50 cells) was counted in five non-overlapping random fields of view (FOVs) under a microscope.

Flow cytometry

The apoptosis of MDA MB 231 and Hs578T cells was monitored by flow cytometry. Briefly, MDA MB 231 and Hs578T cells were collected after transfection for 48 hours and prepared into cell suspension with the concentration of 1×10^6 cells/mL. Later, the Annexin-V-FITC/PI apoptosis kit (C1062M, Beyotime, Shanghai, China) was adopted for cell double staining carried out in strict accordance with the manufacturer's instructions. Afterwards, the percentage of apoptotic cells was assessed by flow cytometry (FACSCalibur, BD Biosciences, San Jose, California, USA).

Transwell assay

The harvested MDA MB 231 and Hs578T cells were prepared as single-cell suspension (cell density, 1×10^6 cells/mL) with FBS-free DMEM. Then, 500 μ L cell suspension was added into the upper chamber of the 6-well inserts (pore size, 8 μ m), whereas 600 μ L DMEM that contained 10% FBS was added into the lower chamber. Thereafter, cells were kept under 37°C and 5% CO₂ conditions for 24 hours. Subsequently, cells on the upper chamber surface were removed using a cotton swab, while those on the lower chamber surface were fixed with 4% paraformaldehyde for 15 min and stained with 0.1% crystal violet for 15 min. The number of migrating cells was counted in five non-overlapping random FOVs under a microscope.

Treatments with cycloheximide (CHX) and protease inhibitor MG132

The transfected MDA MB 231 cells and Hs578T cells (1×10^6 cells) were cultured in the 6-well plates with 1 mL DMEM containing 10% FBS and CHX (50 μ g/mL) for 4, 8 and 12 hours under 37°C and 5% CO₂ conditions, respectively.¹⁹ Additionally, 1 mL DMEM supplemented with 10% FBS and protease inhibitor MG132 (5 μ M) was added to culture cells in the 6-well plates for 24 hours under 37°C and 5% CO₂ conditions.²⁰ Finally, cells were collected to detect the programmed cell death ligand 1 (PD-L1) protein expression by WB assay.

Ubiquitination assay

As previously described, ubiquitination assay was executed to monitor the ubiquitination of PD-L1 protein.^{21 22} Briefly, the transfected MDA MB 231 cells and Hs578T cells were harvested and lysed with the RIPA lysis buffer supplemented with protease inhibitor and phosphatase inhibitor (Beyotime, Shanghai, China) for 1 hour at 4°C. Then, the cell lysate samples were incubated with specific antibody for 2 hours at 4°C, with IgG as the control. The beads were subsequently added into the mixture and

rotated for 12 hours at 4°C. Through centrifugation, the immunoprecipitated complexes were harvested and boiled in the sodium dodecyl sulfate (SDS) loading buffer for 5 min. Later, WB assay was carried out to detect the ubiquitination of PD-L1 protein.

T cell-mediated tumor cell killing assay

The T cell-mediated tumor cell killing assay was performed as described previously.²³ Human CD8+ T cells were purchased from the Shanghai Institute of Cell Biology (Shanghai, China). The activation of CD8+ T cells was completed according to a previous study.²³ MDA MB 231 and Hs578T cells (1×10^6 cells/mL) were cultured in each well of the 96-well plates containing 100 μ L DMEM (10% FBS) under 37°C and 5% CO₂ conditions for 24 hours. Then, MDA MB 231 and Hs578T cells were cocultured with the activated CD8+ T cells for 48 hours. The ratio of CD8+ T cells to MDA MB 231 cells or Hs578T cells was 5:1. At 48 hours later, the residual liquid was removed from each well, and cells were washed with phosphate buffered saline (PBS). Crystal violet (0.1%) was then added into each well to stain cells for 10 min. Finally, the optical density (OD) value was measured at 570 nm using a porous microplate reader (Molecular Devices, Sunnyvale, California, USA).

ELISA

The activation of CD8+ T cells was completed according to previous description.²³ MDA MB 231 cells and Hs578T cells were dispersed in DMEM supplemented with 10% FBS at a density of 1×10^6 cells/mL, and later inoculated into the 6-well plates (1 mL/well) for 24 hours at 37°C and 5% CO₂. Thereafter, MDA MB 231 cells or Hs578T cells were co-cultured with the activated CD8+ T cells for 48 hours in the 6-well plates. The ratio of CD8+ T cells to MDA MB 231 cells or Hs578T cells was 5:1. Afterwards, the coculture medium was collected and centrifuged at 12 000 rpm/min and 4°C for 5 min to obtain the supernatant. Eventually, the levels of IFN γ and IL-2 in the supernatant were detected using the ELISA Kit (Beyotime, Shanghai, China).

Detection of the activated T cell percentage

In brief, MDA MB 231 cells or Hs578T cells were cocultured with the activated CD8+ T cells for 48 hours in the 6-well plates. The ratio of CD8+ T cells to MDA MB 231 cells or Hs578T cells was 5:1. Then, the percentages of CD8+ perforin+ T cells and CD8+ TNF- α + T cells were analyzed by flow cytometry according to previous description.²⁴ To be specific, cells were collected and washed twice with PBS. Then, cells were incubated with the permeabilisation solution (BD Biosciences, San Jose, California, USA) containing PE-Cy7 anti- α -TNF- α (506323, Hengfei Biological Technology Co., Ltd., Shanghai, China) and PerCp-Cy5.5 anti-Perforin (303935, Yubo Biological Technology Co., Ltd., Shanghai, China) for 25 min. Later, CD8+ perforin+ T cells and CD8+ TNF- α + T cells were detected with the flow cytometer (FACSCalibur, BD

Biosciences, San Jose, California, USA). The percentages of CD8⁺ perforin⁺ T cells and CD8⁺ TNF- α ⁺ T cells were analyzed by the FlowJo 9.2 software (Ashland, Oregon, USA).

Dual luciferase reporter gene assay

As predicted based on CircInteractome (<https://circinteractome.nia.nih.gov/>), circ-0000512 contained mutual binding sites for miR-622. Meanwhile, it was predicated based on TargetScan (<http://www.targetscan.org/>) that miR-622 contained mutual binding sites for CMTM6. Therefore, the network among circ-0000512, miR-622 and CMTM6 was investigated by dual luciferase reporter gene assay. The fragments of wild type (WT) and mutant type (MUT) circ-0000512 and CMTM6 were designed and synthesized by Genechem (Shanghai, China). Thereafter, the fragments were cloned and loaded onto the pGL3-luciferase reporter vectors (Promega, Madison, Wisconsin, USA) according to the manufacturer's instructions. Then, pGL3-luciferase reporter vectors were cotransfected with miR-622 mimics or mimics NC into MDA MB 231 cells and Hs578T cells for 48 hours using Lipofectamine 3000. Afterwards, the luciferase activities of MDA MB 231 cells and Hs578T cells were examined with the dual-luciferase reporter assay kit (Promega, Madison, Wisconsin, USA), with renilla luciferase activity as the control.

RNA immunoprecipitation (RIP) assay

To verify the binding of circ-0000512 to miR-622, the Magna RIP kit (Millipore, Bedford, Massachusetts, USA) was used in line with specific instructions in RIP assay. In short, MDA MB 231 and Hs578T cells (1×10^7 cells) were collected and lysed with the RNA lysis buffer (100 μ L). Later, 200 μ L cell lysate was harvested and incubated for 12 hours at 4°C with the RIP immunoprecipitation buffer that contained protein A/G sepharose beads conjugated with IgG antibody (ab171870, Abcam, Shanghai, China) or Ago-2 antibody (ab186733, Abcam, Shanghai, China). Afterwards, the RNeasy Mini Kit (Qiagen, Valencia, California, USA) was employed to extract the immunoprecipitated RNA. Subsequently, cDNA was prepared from RNA through reverse transcription using the reverse transcription kit (Applied Bio-systems, Foster City, California, USA). The immunoprecipitated circ-0000512 and miR-622 levels were determined by qRT-PCR.

In the RIP assay to verify the binding of circ-0000512 to PD-L1 protein, 200 μ L cell lysate was incubated for 12 hours at 4°C with RIP immunoprecipitation buffer that contained magnetic beads conjugated with anti-IgG or PD-L1 antibody. Later, the beads were treated with 0.5 mg/mL proteinase K (Beyotime, Shanghai, China) for 30 min at 55°C to remove proteins. As described above, the extraction, reverse transcription and quantification of circ-0000512 were performed sequentially.

In vivo study

The animal experiments in this study were approved by the Animal Ethics Committee and performed following the Guide for the Care and Use of Laboratory Animals (IRB number: AIRB-2019-1029).

Female BALB/c immunodeficient nude mice (5 weeks old, n=10) and normal immune mice (5 weeks old, n=10) were commercially provided by Shanghai Experiment Animal Center of the Chinese Academy of Sciences (Shanghai, China). Then, mice were housed in a room under (22 \pm 1)°C and 12 hours/12 h day/night cycle conditions. Food and water were both freely available.

Using Lipofectamine 3000, MDA MB 231 cells and 4T1 cells (Shanghai Institute of Cell Biology, Shanghai, China) were transfected with shRNA targeting circ-0000512 and the corresponding NC, respectively. After transfection, cells were separately dispersed into PBS to a concentration of 1×10^7 cells/mL. Later, 100 μ L cell suspensions was collected and subcutaneously injected into the mammary fat pad of mice. The transfected MDA MB 231 cells were respectively injected into immunodeficient nude mice with five mice per group, while 4T1 cells were respectively injected into normal immune mice with five mice per group. Tumor size was measured at intervals of 7 days for 28 consecutive days. Meanwhile, tumor volume was calculated by $V = (\text{long diameter} \times \text{short diameter}^2) / 2$. On day 28, mice were euthanized to collect the tumors. After dissection, tumors were weighted and stored at -80°C.

Immunohistochemistry (IHC)

CD8⁺T cells in xenograft tumor tissues of mice were evaluated by IHC. In brief, xenograft tumor tissues were processed with fixation and paraffin embedding in sequence in accordance with the standard procedures. Thereafter, xenograft tumor tissues were prepared into 5 μ m sections. After deparaffinization and rehydration, the sections were treated with 3% H₂O₂ for 15 min and then with 5% normal goat serum for 10 min. Subsequently, rabbit anti-CD8 primary antibody (1:100, ab85792, Abcam, Shanghai, China) was evenly dripped onto each section to probe for 12 hours at 4°C. Thereafter, the horseradish peroxidase (HRP)-labeled antirabbit secondary antibody (1:200, ab6721, Abcam, Shanghai, China) was added to incubate the sections for 30 min. Later, 3,3'-diaminobenzidine tetrahydrochloride was added for color developing for 10 min. After dehydration and transparentizing, the sections were sealed in neutral resin. At last, CD8⁺T cells were presented as brown particles under the microscope. qRT-PCR

Total cellular or tissue RNAs were isolated with the Trizol reagent. Afterwards, the cDNA templates were synthesized using a PrimeScript RT Reagent Kit (Takara, Dalian, China) according to specific instructions. qRT-PCR assay was performed using a SYBR Premix Ex Taq II Kit (TaKaRa, Dalian, China) on the StepOnePlus real-time PCR system (Applied Biosystems, Foster City, California, USA). The primers used in this experiment are shown below:

For circ_0000520, 5'-GTCTGAGACTAGGGCC AGAGGC-3' (forward), 5'-GACATGGGAGTGGAGT GACAGG-3' (reverse); for circ_0000518, 5'-CTAACAG-GGCTCTCCCTGAG-3' (forward), 5'-CAGACCTTC-CCAAGGGACAT-3' (reverse); for circ_0000514, 5'-CTGCCCAGTCTGACCTCG-3' (forward), 5'-C-CGTTTCCTCCGTAGGCG-3' (reverse); for circ_0000511, 5'-CCTCCTTTGCCGGAGCTT-3' (forward), 5'-GGTC-CACGGCATCTCCTG-3' (reverse); for circ_0000512, 5'-GGAACAGACTCACGGCCA-3' (forward), 5'-CATCTCCTGCCAGTCTGAC-3' (reverse); for Cyclin D1 (CCND1), 5'-AGAGGCGGAGGAGAACA-3' (forward), 5'-GAGAGGAAGCGTGTGAGG-3' (reverse); for B-cell lymphoma/leukemia 2, 5'-GCGGATTG-ACATTTCTGTG-3' (forward), 5'-CATAAGGCAAC-GATCCCA-3' (reverse); for cyclin-dependent kinase inhibitor 1A (CDKN1A), 5'-ATGAGTTGGGAG-GAGGCA-3' (forward), 5'-CTGAGCGAGGCACAAGG-3' (reverse); for early two factor transcription factor 1 (E2F1), 5'-GGGTTTCCAGAGATGCTCA-3' (forward), 5'-CCTTCTGCTTGGCTTGTCTCA-3' (reverse); for MYC, 5'-G-CCAGAGGAGGAACGAG-3' (forward), 5'-GCTTGGAC-GGACAGGAT-3' (reverse); for proliferating cell nuclear antigen (PCNA), 5'-GCCTGACAAATGCTTGCT-3' (forward), 5'-GCGGGAAGGAGGAAAGT-3' (reverse); for C-X-C motif chemokine ligand 10 (CXCL10), 5'-AAGCAGTTAGCAAGGAAAGG-3' (forward), 5'-GTAGG-GAAGTGATGGGAGAG-3' (reverse); for C-C chemokine ligand 2 (CCL2), 5'-TTTTCCCCTAGCTTTCCC-3' (forward), 5'-GCAATTTCCCCAAGTCTCT-3' (reverse). For interleukin-2 (IL2), forward, 5'-GAATGGAATTAA TAATTACAAGAATCCC-3' (forward), 5'-TGTTTCAG ATCCCTTTAGTTCCAG-3' (forward). For interferon gamma (IFNG), 5'-GCATCGTTTGGGTTCTCT-3' (forward), 5'-CGCTACATCTGAATGACCTG-3' (reverse); for signal transducers and activators of transcription 1 (STAT1), 5'-TGCTCCCTCTCTGGAATG-3' (forward), 5'-CTCCTTGCTGATGAAGCC-3' (reverse); for chemokine-like factor super family member 6 (CMTM6), 5'-GCAACAATATCAGCAACTTCGT-3' (forward), 5'-TTGGTCCTTAGGTGTGGTATCA-3' (reverse); for PD-L1, 5'-CACCACCACCAATTCCAAGAG-3' (forward), 5'-AGGATGTGCCAGAGGTAGTTC-3' (reverse); for Actin, 5'-GTGGGCCGCTCTAGGCACCA-3' (forward), 5'-CGGTTGGCCTTAGGGTTCAGGGGGG-3' (reverse); for miR-622, 5'-ATCCCAGGGAGACAGAGATCGAGG-3' (forward), 5'-AAGCTTGGTGGTGGACTTTTGGTTGT-3' (reverse); for U6, 5'-CTCGCTTCGGCAGCATATACT-3' (forward), 5'-ACGCTTCACGAATTTGCGTGTC-3' (reverse). The reaction conditions were as follows: 95°C for 2 min, followed by 40 cycles of 95°C for 10 s and 60°C for 40 s. Using the $2^{-\Delta\Delta C_t}$ method, the relative expression of miR-622 was normalized to U6, while that of the other genes was normalized to Actin.

Western blotting (WB) assay

Total cellular or tissue proteins were extracted using the RIPA lysis buffer (Beyotime, Shanghai, China). To

be specific, tissues were ground into powder in liquid nitrogen before they were incubated with RIPA lysis buffer. Later, the total protein concentration was investigated using a BCA kit (Beyotime, Shanghai, China). Equivalent amounts of total protein samples were separated by SDS-polyacrylamide gel electrophoresis and transferred onto polyvinylidene fluoride membranes. Later, the membranes were blocked with 5% skimmed milk for 1 hour at room temperature and incubated with primary antibodies overnight at 4°C. The primary antibodies used in this study are listed below: rabbit anti-PD-L1 (1:1000, ab213480, Abcam, Shanghai, China), anti-CMTM6 (1:1000, ab264067, Abcam, Shanghai, China), anti-COP9 signalosome 5 (CSN5) (1:1000, ab195635, Abcam, Shanghai, China) and anti-Actin (1:1000, Abcam, Shanghai, China). After washing with Tris-buffered saline containing 0.05% Tween 20 (TBST), membranes were further incubated with HRP-conjugated antirabbit secondary antibody (1:2000, ab6721, Abcam, Shanghai, China) for 2 hour at room temperature. At last, the protein blots were visualized using a chemiluminescence reagent kit (Millipore, Billerica, Massachusetts, USA) according to specific instructions. The gray value of each blot was quantified by the ImageJ software (NIH, Bethesda, Maryland, USA), with actin being the control.

Statistical analysis

The experiments were performed in triplicate independently. All data were presented in the form of mean±SD. Two-tailed Student's t-test or one-way ANOVA was respectively performed for the comparison between two groups or more than two groups. Data were analyzed by the Graphpad Prism V.6.0 software. The correlation analysis of circ-0000512, miR-622 and CMTM6 expression in TNBC tissues was performed by Pearson correlation analysis. $P < 0.05$ indicated statistical significance.

RESULTS

circ-0000512 knockdown attenuated the proliferation and migration of TNBC cells and enhanced their apoptosis

Analysis based on GEO database revealed five upregulated circRNAs (including circ-0000520, circ-0000518, circ-0000514, circ-0000511 and circ-0000512) and five downregulated circRNAs (namely, circ-103345, circ-104270, circ-102051, circ-102619 and circ-102049) in TNBC (figure 1A). This study focused on the five upregulated circRNAs. To this end, we first measured the expression of 5 upregulated circRNAs in patients with TNBC and cells by qRT-PCR. In patients with TNBC, circ-0000520, circ-0000518, circ-0000514, circ-0000511 and circ-0000512 were all significantly overexpressed in tumor tissues than that in adjacent normal tissues ($p < 0.05$ or $p < 0.01$) (figure 1B). Among the five upregulated circRNAs, the expression levels of circ-0000518 and circ-0000512 were higher than those of the other three circRNAs. Meanwhile, circ-0000518 has been studied in previous work. Therefore, this study selected circ-0000512

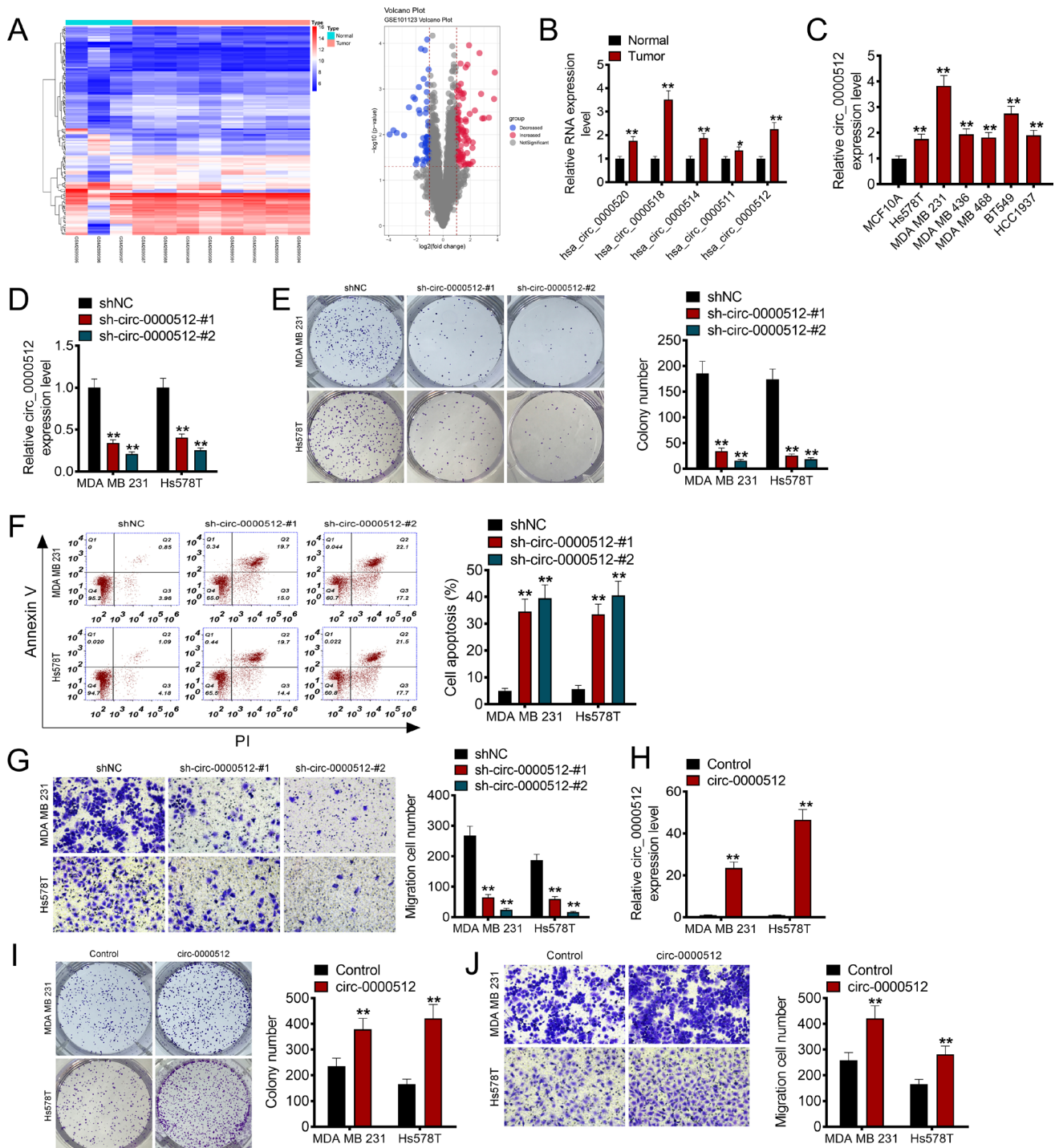


Figure 1 circ-0000512 knockdown attenuated TNBC cells proliferation, migration and enhanced apoptosis. (A) Differentially expressed circRNAs analysis in TNBC by GEO data analysis. (B) The upregulated circRNAs expression detection in patients with TNBC by qRT-PCR. * $P < 0.05$ or ** $P < 0.01$ vs adjacent normal tissues. (C) circ-0000512 expression in cell lines by qRT-PCR. ** $P < 0.01$ vs MCF10A cell line. (D) circ-0000512 expression in MDA MB 231 and Hs578T cells transfected by circ-0000512 shRNA and NC as researched by qRT-PCR. ** $P < 0.01$ vs shNC group. (E) Proliferation of MDA MB 231 and Hs578T cells transfected by circ-0000512 shRNA and NC as explored by colony formation assay. ** $P < 0.01$ vs shNC group. (F) Apoptosis of MDA MB 231 and Hs578T cells transfected by circ-0000512 shRNA and NC as investigated by flow cytometry. ** $P < 0.01$ vs shNC group. (G) Migration of MDA MB 231 and Hs578T cells transfected by circ-0000512 shRNA and NC as assessed by Transwell experiment. ** $P < 0.01$ vs shNC group. (H) circ-0000512 expression in MDA MB 231 and Hs578T cells transfected by circ-0000512 vector and empty vector as researched by qRT-PCR. ** $P < 0.01$ vs Control group. (I) Proliferation of MDA MB 231 and Hs578T cells transfected by circ-0000512 vector and empty vector as explored by colony formation assay. ** $P < 0.01$ vs Control group. (J) Migration of MDA MB 231 and Hs578T cells transfected by circ-0000512 vector and empty vector as evaluated by Transwell experiment. ** $P < 0.01$ vs Control group. GEO, Gene Expression Omnibus; NC, negative control; qRT-PCR, quantitative reverse transcription PCR; TNBC, triple-negative breast cancer.

for follow-up research. From [figure 1C](#), consistent with the result obtained from human breast epithelial cell line (MCF10A), circ-0000512 was markedly overexpressed in six TNBC cell lines (Hs578T, MDA MB 231, MDA MB 436, MDA MB 468, BT549 and HCC1937) ($p < 0.01$). All of these data revealed that circ-0000512 was upregulated in patients with TNBC and cells.

As observed from [figure 1C](#), the highest and lowest circ-0000512 levels were detected in MDA MB 231 and Hs578T cell lines, respectively. Thus, MDA MB 231 and Hs578T cell lines were used as the objects in the following research. Then, knockdown or overexpression of circ-0000512 was achieved in the two cell lines through transfection.

It was observed from [figure 1D](#) that circ-0000512 expression significantly decreased in MDA MB 231 and Hs578T cells of sh-circ-0000512-#1 group and sh-circ-0000512-#2 group compared with that of shNC group ($p < 0.01$). Later, colony formation assay, flow cytometry and Transwell assays were performed to detect cell proliferation, apoptosis and migration. As a result, MDA MB 231 and Hs578T cells of sh-circ-0000512-#1 group and sh-circ-0000512-#2 group displayed a prominently lower colony number, a higher apoptotic rate and a lower number of migrating cells compared with those of shNC group ($p < 0.01$) ([figure 1E–G](#)).

Additionally, circ-0000512 expression in MDA MB 231 and Hs578T cells of circ-0000512 group increased relative to that of Control group ($p < 0.01$) ([figure 1H](#)). Moreover, markedly higher colony numbers and migrating cell numbers were observed in MDA MB 231 and Hs578T cells of circ-0000512 group relative to those of Control group ($p < 0.01$) ([figure 1I,J](#)).

circ-0000512 knockdown inhibited PD-L1 protein expression in TNBC cells by promoting its ubiquitination

The mRNAs levels of genes related to cell proliferation (CCND1, BCL2, CDKN1A, E2F1, MYC and PCNA) and immune escape (PD-L1, CXCL10, CCL2, IL2, IFNG and STAT1) were detected by qRT-PCR. According to [figure 2A,B](#), relative to Control group, the CCND1, BCL2, E2F1, MYC and PCNA mRNA levels increased in MDA MB 231 and Hs578T cells of circ-0000512 group, whereas CDKN1A, CXCL10, CCL2, IL2, IFNG and STAT1 mRNA levels decreased ($p < 0.05$ or $p < 0.01$). Compared with shNC group, MDA MB 231 and Hs578T cells of sh-circ-0000512-#1 group and sh-circ-0000512-#2 group showed much lower CCND1, BCL2, E2F1, MYC and PCNA mRNA levels, whereas higher CDKN1A, CXCL10, CCL2, IL2, IFNG and STAT1 mRNA levels ($p < 0.01$). However, PD-L1 mRNA expression in MDA MB 231 and Hs578T cells was not significantly affected by circ-0000512 upregulation or downregulation. Interestingly, WB assay exhibited that, MDA MB 231 and Hs578T cells of circ-0000512 group expressed significantly higher PD-L1 protein levels than those of Control group. On the contrary, MDA MB 231 and Hs578T cells of sh-circ-0000512-#1 group and sh-circ-0000512-#2 group expressed lower PD-L1 protein

levels than those of shNC group ($p < 0.01$) ([figure 2C](#)). Thus, it was speculated that circ-0000512 might affect PD-L1 expression at protein level but not mRNA level.

As suggested by RIP assay, circ-0000512 was not precipitated by PD-L1 protein. Therefore, there was no direct binding interaction between circ-0000512 and PD-L1 protein ([figure 2D](#)). Subsequently, MDA MB 231 and Hs578T cells were treated with the protein synthesis inhibitor (CHX). As a result, circ-0000512 knockdown obviously declined the half-life of PD-L1 protein in MDA MB 231 and Hs578T cells ([figure 2E](#)). Thereafter, the proteasome inhibitor (MG-132) was applied to treat MDA MB 231 and Hs578T cells. As observed from [figure 2F](#), MDA MB 231 and Hs578T cells treated with MG-132 exhibited higher PD-L1 protein levels than those without MG-132 treatment. Interestingly, circ-0000512 knockdown did not obviously affect the PD-L1 protein level in MDA MB 231 and Hs578T cells. Therefore, circ-0000512 knockdown inhibited PD-L1 protein level by destroying its stability. Based on results from ubiquitination assay, circ-0000512 knockdown prominently promoted the PD-L1 protein ubiquitination level ([figure 2G](#)). These data demonstrated that circ-0000512 knockdown destroyed the PD-L1 protein stability by promoting its ubiquitination.

circ-0000512 knockdown enhanced PD-L1 protein ubiquitination modification in TNBC cells by inhibiting CMTM6 expression

According to a previous study, CMTM6 and CSN5 have the function of inhibiting the ubiquitination of PD-L1 protein.²⁵ Thus, in order to explore the depth molecular mechanisms by which circ-0000512 promotes TNBC progression, this study researched the expression of CMTM6 and CSN5 in the circ-0000512 silenced-TNBC or circ-0000512 overexpressed-TNBC cells. The mRNA and protein expression levels of CMTM6 and CSN5 in MDA MB 231 and Hs578T cells were detected by qRT-PCR and WB assays. Compared with Control group, the CMTM6 protein and mRNA expression levels in MDA MB 231 and Hs578T cells of circ-0000512 group significantly increased ($p < 0.01$). Conversely, relative to shNC group, the CMTM6 protein and mRNA expression levels distinctly decreased in MDA MB 231 and Hs578T cells of sh-circ-0000512-#1 group and sh-circ-0000512-#2 group ($p < 0.01$). However, CSN5 protein and mRNA expression levels were not obviously changed by circ-0000512 upregulation or downregulation ([figure 3A,B](#)). These data implied that circ-0000512 could promote the expression of CMTM6 (rather than CSN5). Therefore, in the following study, CMTM6 was selected as the subject.

Next, the function of CMTM6 on the ubiquitination of PD-L1 protein in TNBC cells was verified. Compared with shNC group, CMTM6 protein and mRNA levels, and PD-L1 protein level significantly decreased in MDA MB 231 and Hs578T cells of sh-CMTM6 group ($p < 0.01$). Oppositely, in comparison with Control group, the CMTM6 protein and mRNA levels, and PD-L1 protein level were markedly increased in MDA

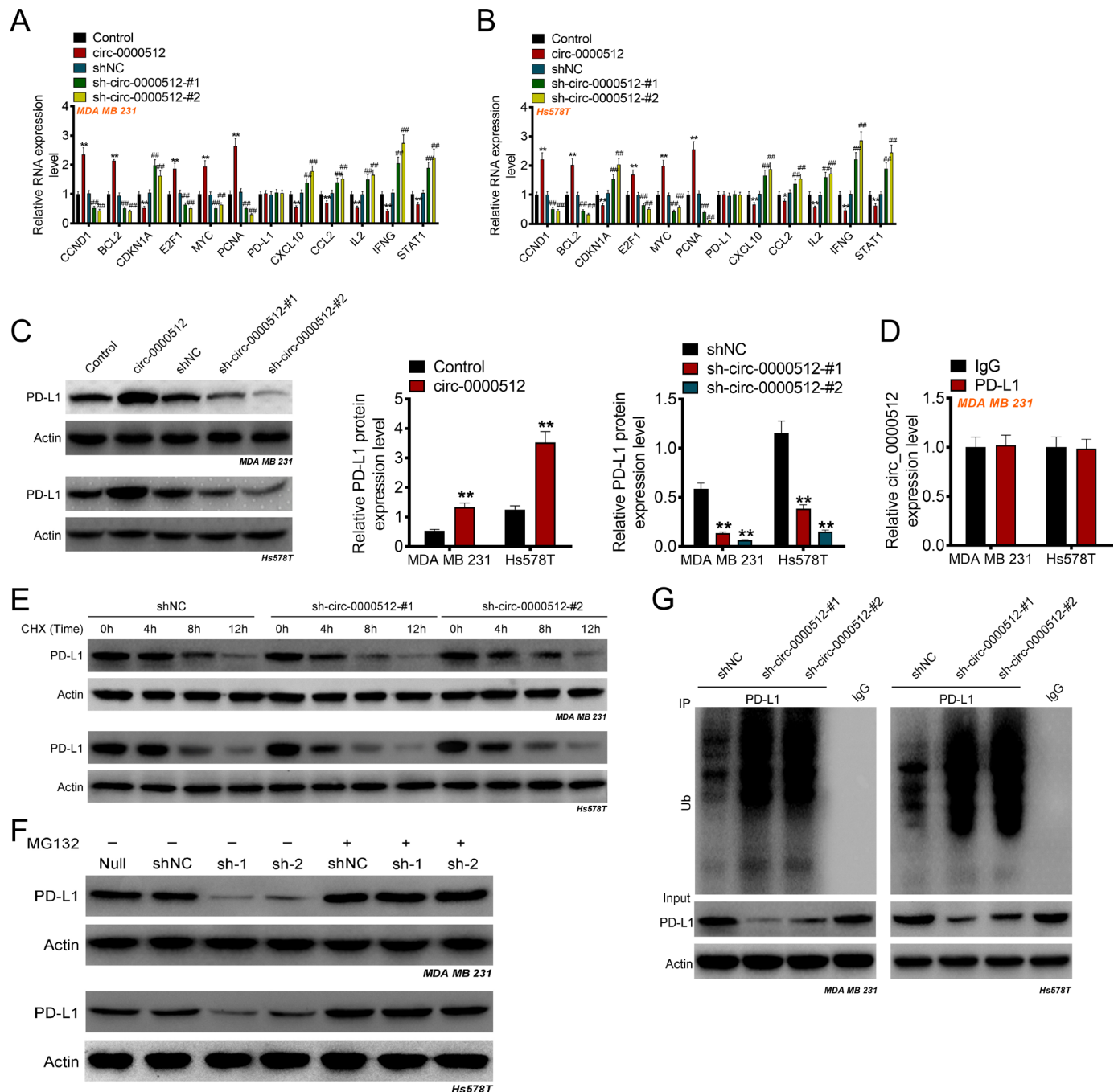


Figure 2 circ-0000512 knockdown inhibited PD-L1 protein expression in TNBC cells by promoting its ubiquitination. (A and B) The mRNAs levels of genes related to cell proliferation (CCND1, BCL2, CDKN1A, E2F1, MYC and PCNA) and immune escape (PD-L1, CXCL10, CCL2, IL2, IFNG and STAT1) in MDA MB 231 and Hs578T cells as detected by qRT-PCR. * $P < 0.05$ or ** $p < 0.01$ vs Control group. ### $P < 0.01$ vs shNC group. (C) PD-L1 protein expression in MDA MB 231 and Hs578T cells as researched by Western blot. ** $P < 0.01$ vs Control group or shNC group. (D) circ-0000512 precipitation by PD-L1 protein in MDA MB 231 and Hs578T cells as assessed by RIP assay. (E) After protein synthesis inhibitor (CHX) treatment, PD-L1 protein expression in MDA MB 231 and Hs578T cells as researched by Western blot. (F) After proteasome inhibitor (MG-132) treatment, PD-L1 protein expression in MDA MB 231 and Hs578T cells as evaluated by Western blot. (G) The ubiquitination of PD-L1 protein in MDA MB 231 and Hs578T cells as explored by Western blot. NC, negative control; qRT-PCR; quantitative reverse transcription PCR; RIP, RNA immunoprecipitation; TNBC, triple-negative breast cancer.

MB 231 and Hs578T cells of CMTM6 group ($p < 0.01$). However, PD-L1 mRNA levels in MDA MB 231 and Hs578T cells were not obviously affected by CMTM6 upregulation or downregulation (figure 3C,D). In

this regard, CMTM6 promoted PD-L1 expression at protein level but not mRNA level.

CHX and MG-132 were used respectively to treat MDA MB 231 and Hs578T cells. According to

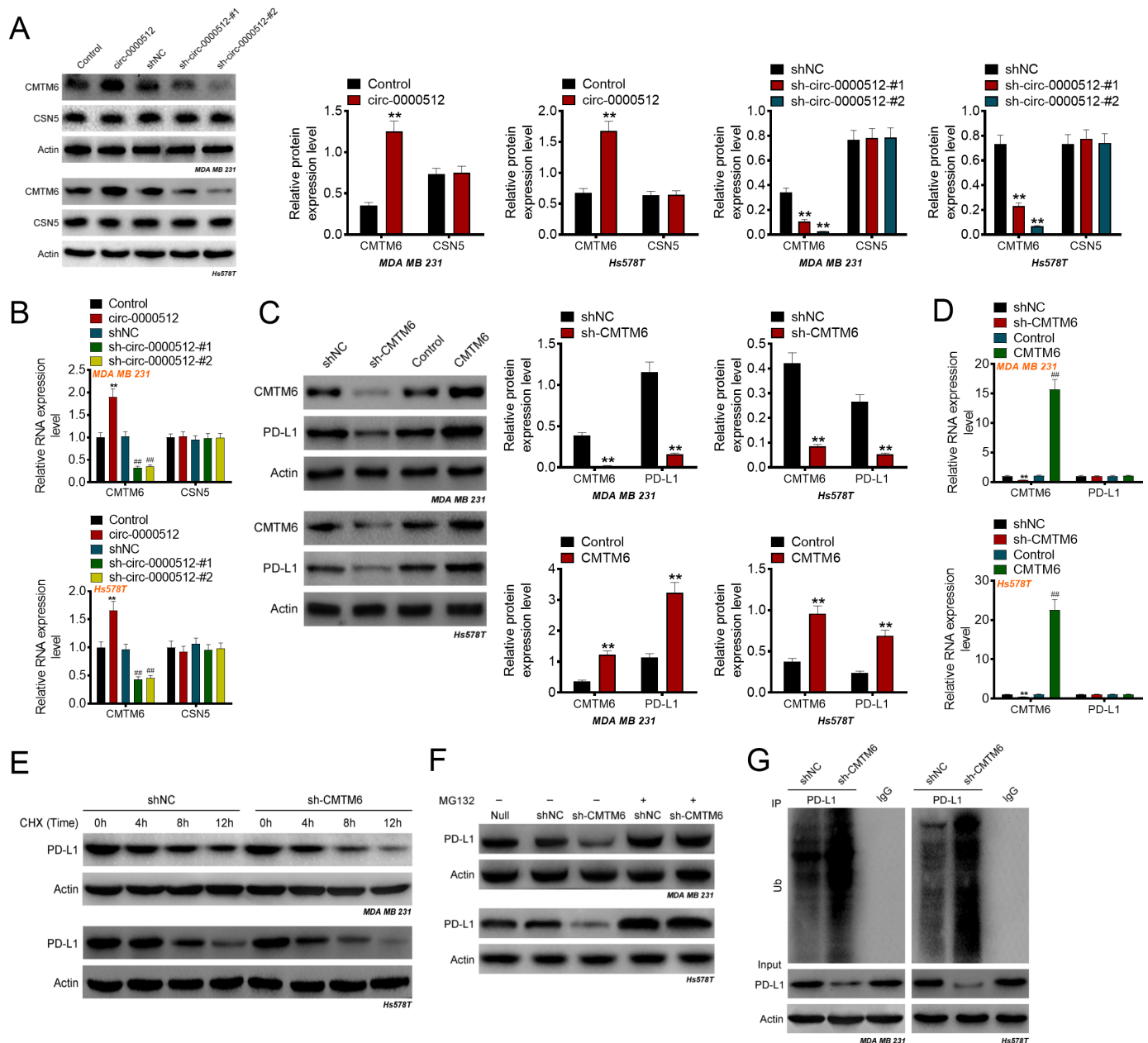


Figure 3 circ-0000512 knockdown enhanced PD-L1 protein ubiquitination modification in TNBC cells through inhibiting CMTM6 expression. (A) CMTM6 and CSN5 proteins expression in MDA MB 231 and Hs578T cells as assessed by Western blot. **P<0.01 vs Control group or shNC group. (B) CMTM6 and CSN5 mRNAs expression in MDA MB 231 and Hs578T cells as researched by qRT-PCR. **P<0.01 vs Control group. ##P<0.01 vs shNC group. (C) CMTM6 and PD-L1 proteins expression in MDA MB 231 and Hs578T cells as explored by Western blot. **P<0.01 vs Control group or shNC group. (D) CMTM6 and PD-L1 mRNAs expression in MDA MB 231 and Hs578T cells as investigated by qRT-PCR. **P<0.01 vs shNC group. ##P<0.01 vs Control group. (E) After protein synthesis inhibitor (CHX) treatment, PD-L1 protein expression in MDA MB 231 and Hs578T cells as researched by Western blot. (F) After proteasome inhibitor (MG-132) treatment, PD-L1 protein expression in MDA MB 231 and Hs578T cells as evaluated by Western blot. (G) The ubiquitination of PD-L1 protein in MDA MB 231 and Hs578T cells as explored by Western blot. NC, negative control; qRT-PCR; quantitative reverse transcription PCR; TNBC, triple-negative breast cancer.

figure 3E,F, CMTM6 knockdown obviously shortened the half-life of PD-L1 protein. Moreover, MG-132 treatment increased the PD-L1 protein expression in MDA MB 231 and Hs578T cells. Thus, CMTM6 knockdown destroyed the stability of PD-L1 protein. Ubiquitination assay displayed that, CMTM6 knockdown increased the ubiquitination level of PD-L1 protein

(figure 3G). These data revealed that CMTM6 knockdown reduced the PD-L1 protein level by enhancing its ubiquitination. Consequently, circ-0000512 knockdown might enhance PD-L1 protein ubiquitination through inhibiting CMTM6 expression.

circ-0000512 promoted CMTM6 expression by sponging miR-622 in TNBC

By analysis based on Circular RNA Interactome, nine miRNAs were found to be interacted with circ-0000512, including miR-622. Meanwhile, according to miRDB-based analysis, 96 miRNAs were discovered to be interacted with CMTM6, including miR-622. Notably, miR-622 was the only miRNA that interacted with circ-0000512 and CMTM6, which was thereby selected as the research object.

The binding site between circ-0000512 and miR-622 is displayed in [figure 4A](#). Dual luciferase reporter gene assay was performed on MDA MB 231 and Hs578T cells. As a result, miR-622 upregulation markedly reduced the luciferase activity of circ-0000512-WT ($p < 0.01$), but did not obviously change that of circ-0000512-MUT ([figure 4B](#)). RIP assay demonstrated that both miR-622 and circ-0000512 in MDA MB 231 and Hs578T cells were significantly precipitated by anti-Ago2 ($p < 0.01$) ([figure 4C](#)). Furthermore, circ-0000512 upregulation suppressed the expression of miR-622, whereas circ-0000512 downregulation elevated the expression of miR-622 in MB 231 and Hs578T cells ($p < 0.01$) (online supplemental figure 1A,B). Therefore, circ-0000512 could directly repress the expression of miR-622.

The binding site between miR-622 and CMTM6 is shown in [figure 4D](#). According to the results, miR-622 upregulation distinctly declined the luciferase activity of CMTM6-WT in MDA MB 231 and Hs578T cells ($p < 0.01$). However, miR-622 upregulation did not obviously change the luciferase activity of CMTM6-MUT in MDA MB 231 and Hs578T cells. Hence, CMTM6 directly bound to miR-622 ([figure 4E](#)).

WB assay exhibited that, compared with NC group, the CMTM6 protein level in MDA MB 231 and Hs578T cells of miR-622 mimics group significantly decreased ($p < 0.01$) ([figure 4F,G](#)). Besides, high CMTM6 protein expression was detected in tumor tissues of patients with TNBC relative to that in adjacent normal tissues ($p < 0.01$) ([figure 4H](#)). In contrast to adjacent normal tissues, high CMTM6 mRNA expression and low miR-622 expression were detected in tumor tissues ($p < 0.01$) ([figure 4I](#)). Simultaneously, in tumor tissues of patients with TNBC, the expression of circ-0000512 was negative correlated with miR-622 ($p = 0.0267$), but positively correlated with CMTM6 ($p = 0.0072$) (online supplemental figure 2A,B). All of these results illustrated that circ-0000512 promoted CMTM6 expression in TNBC by sponging miR-622.

circ-0000512 knockdown enhanced the T cell killing ability in TNBC

In brief, CD8⁺ T cells were cocultured with MDA MB 231 and Hs578T cells. Thereafter, the levels of IFN γ and IL2 in the supernatant of coculture medium were analyzed by ELISA. Relative to shNC group, MDA MB 231 and Hs578T cells of sh-circ-0000512-#1 group and sh-circ-0000512-#2 group presented much higher IFN γ and IL2 levels in the supernatant of co-culture medium

($p < 0.01$) ([figure 5A,B](#)). Flow cytometry revealed that, compared with shNC group, sh-circ-0000512-#1 group and sh-circ-0000512-#2 group displayed distinctly higher percentages of CD8⁺perforin⁺T cells and CD8⁺TNF- α ⁺T cells ($p < 0.01$) ([figure 5C,D](#)). Simultaneously, MDA MB 231 and Hs578T cells of sh-circ-0000512-#1 group and sh-circ-0000512-#2 group exhibited remarkably lower OD values than that of shNC group ($p < 0.01$) ([figure 5E](#)).

circ-0000512 knockdown inhibited TNBC cell growth both in immunodeficient mice and normal immune mice

In brief, MDA MB 231 cells were injected into immunodeficient nude mice. As a result, circ-0000512 knockdown resulted in the significantly decreased xenograft tumor volume and weight ($p < 0.01$) ([figure 6A,B](#)). In comparison with shNC group, xenograft tumor tissues of sh-circ-0000512 group presented remarkably lower circ-0000512 expression, higher miR-622 expression as well as lower CMTM6 mRNA and protein expression ($p < 0.01$) ([figure 6C,D](#)).

Additionally, 4T1 cells were injected into normal immune mice for in vivo study. As shown in [figure 6E,F](#), circ-0000512 knockdown markedly reduced the growth of 4T1 cells in vivo ($p < 0.01$). Compared with shNC group, xenograft tumor tissues of sh-circ-0000512 group displayed lower circ-0000512 expression, higher miR-622 expression, together with lower CMTM6 mRNA and protein expression ($p < 0.01$). Meanwhile, circ-0000512 knockdown did not significantly affect the PD-L1 mRNA expression, but markedly reduced the PD-L1 protein expression in xenograft tumor tissues ($p < 0.01$) ([figure 6G,H](#)). CD8⁺ T cells in xenograft tumor tissues of normal immune mice were detected by IHC. As exhibited in [figure 6I](#), more CD8⁺ T cells were observed in sh-circ-0000512 group than those in shNC group.

DISCUSSION

The present work was the first to explore the function of circ-0000512 in TNBC progression. It was revealed that circ-0000512 was aberrantly upregulated in patients with TNBC and cells. In terms of the underlying mechanism, circ-0000512 might inhibit PD-L1 ubiquitination through sponging the miR-622/CMTM6 axis, thus promoting TNBC progression and immune escape. The intuitive molecular mechanism is presented in [figure 7](#).

At present, data regarding the effect of circ-0000512 on human diseases are still lacking. This study exactly revealed that circ-0000512 knockdown attenuated the proliferation and migration of TNBC cells and enhanced their apoptosis. qRT-PCR assay revealed that circ-0000512 knockdown reduced the mRNA levels of CCND1, BCL2, E2F1, MYC and PCNA, and elevated those of CDKN1A, CXCL10, CCL2, IL2, IFNG and STAT1. By contrast, circ-0000512 overexpression had opposite effects. CCND1, BCL2, E2F1, MYC and PCNA are the well-known oncogenes, which facilitate tumorigenesis and progression through multiple approaches, such as promotion of cell

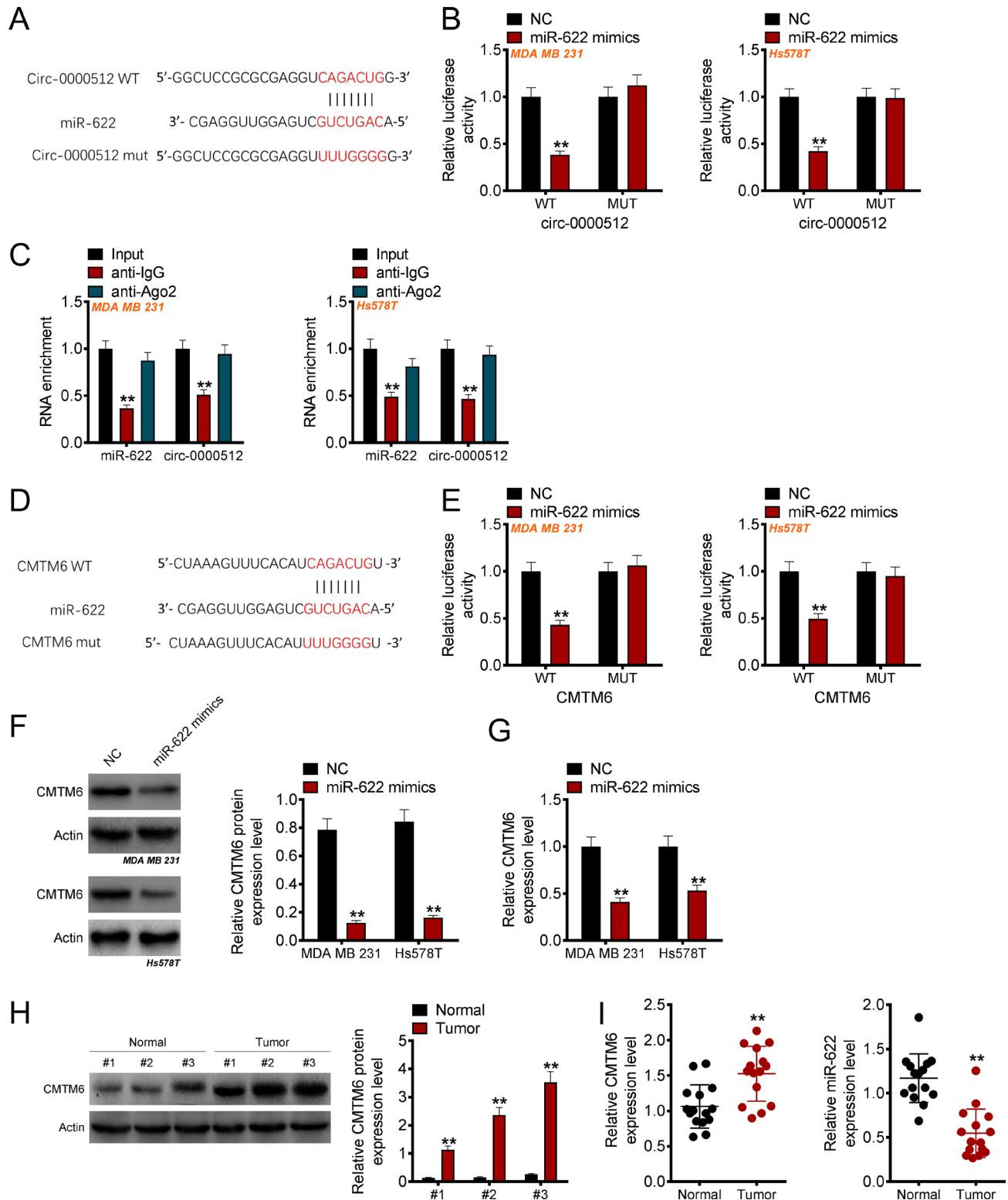


Figure 4 circ-0000512 promoted CMTM6 expression by sponging miR-622 in TNBC. (A) The binding site between circ-0000512 and miR-622. (B) The targeting relationship between circ-0000512 and miR-622 as researched by dual luciferase reporter gene assay. ** $P < 0.01$ vs NC group. (C) circ-0000512 and miR-622 precipitation in MDA MB 231 and Hs578T cells as reflected by RIP assay. ** $P < 0.01$ vs anti-Ago2 group. (D) The targeting relationship between miR-622 and CMTM6 as explored by dual luciferase reporter gene assay. ** $P < 0.01$ vs NC group. (E) CMTM6 protein expression in MDA MB 231 and Hs578T cells as investigated by Western blot. ** $P < 0.01$ vs NC group. (F) CMTM6 mRNA expression in MDA MB 231 and Hs578T cells as researched by qRT-PCR. ** $P < 0.01$ vs NC group. (G) CMTM6 protein expression in patients with TNBC as assessed by Western blot. ** $P < 0.01$ vs adjacent normal tissues. (H) CMTM6 mRNA and miR-622 expression in patients with TNBC as evaluated by qRT-PCR. ** $P < 0.01$ vs adjacent normal tissues. NC, negative control; qRT-PCR; quantitative reverse transcription PCR; TNBC, triple-negative breast cancer.

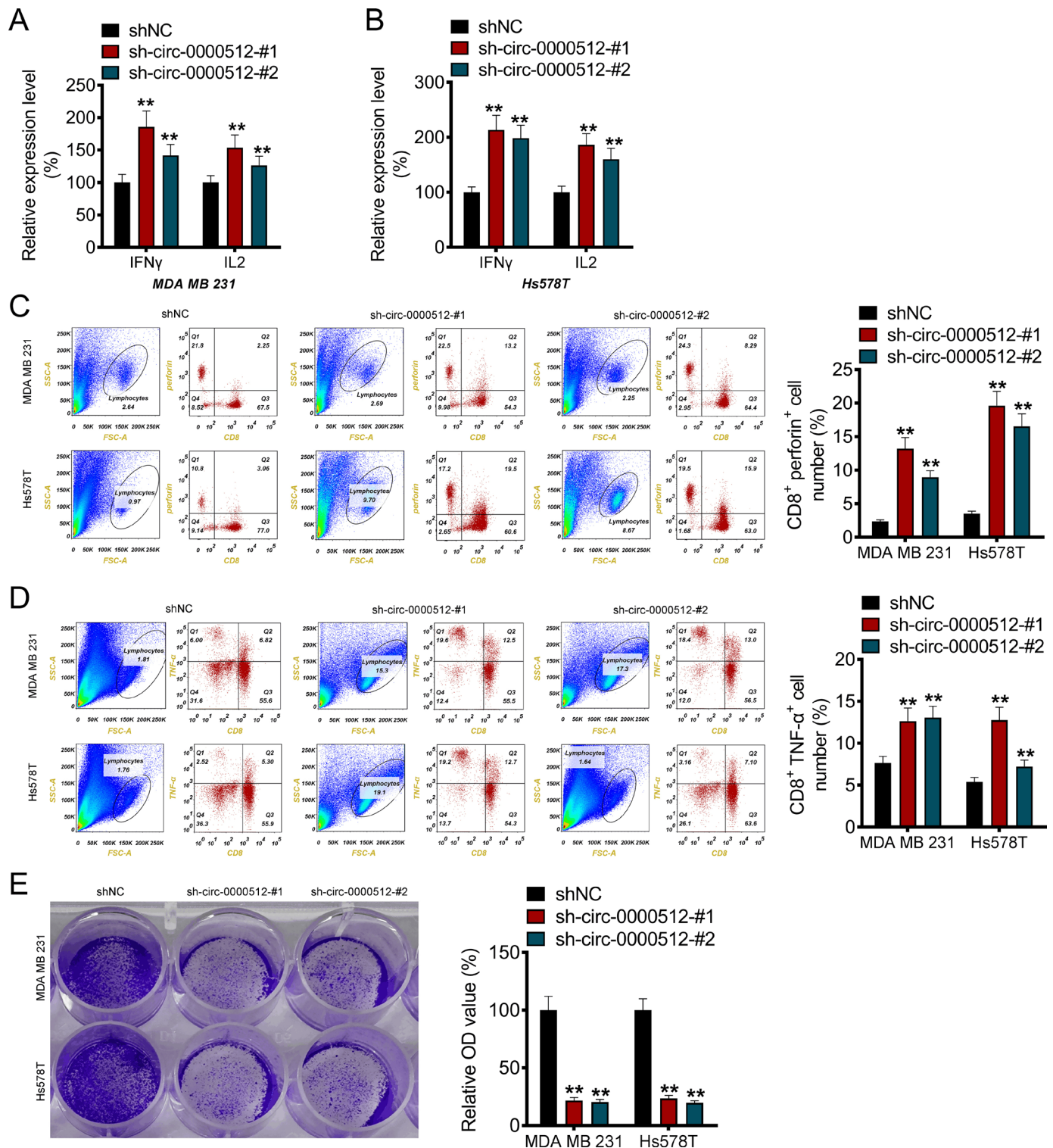


Figure 5 circ-0000512 knockdown enhanced T cell killing ability in TNBC. (A,B) CD8 $^{+}$ T cells were cocultured with MDA MB 231 and Hs578T cells. IFN γ and IL2 level in the coculture medium supernatant was detected using ELISA. (C,D) The percentage of CD8 $^{+}$ perforin $^{+}$ T cells and CD8 $^{+}$ TNF- α $^{+}$ T cells as assessed by flow cytometry. (E) MDA MB 231 and Hs578T cells viability as researched by crystal violet staining. ** $P < 0.01$ vs shNC group. NC, negative control; TNBC, triple-negative breast cancer.

cycle progression from G1 phase to S phase, apoptosis repression, proliferation and metastasis induction.^{26–30} On the contrary, CDKN1A is confirmed as a tumor-suppressor gene due to its activities of proliferation repression and apoptosis induction.³¹ Therefore, in this

study, circ-0000512 knockdown might inhibit the malignant phenotypes of TNBC by downregulating CCND1, BCL2, E2F1, MYC and PCNA and upregulating CDKN1A. Immune escape is a classic feature of tumorigenesis and progression. Tumor cells can avoid T cells capture and

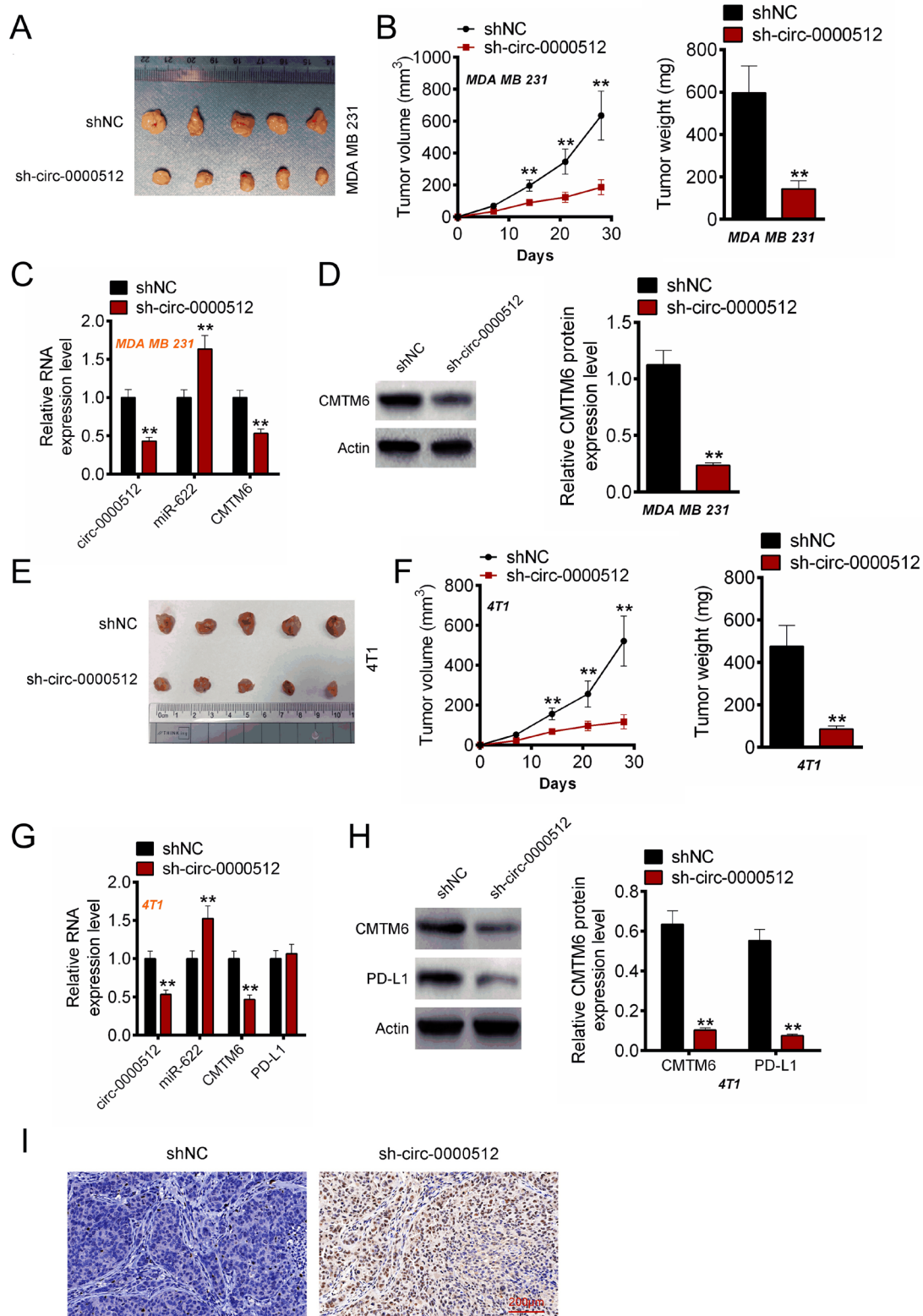


Figure 6 circ-0000512 knockdown inhibited TNBC cells growth both in immunodeficient mice and normal immune mice. (A) The image of xenograft tumor tissues in immunodeficient nude mice. (B) Xenograft tumor volume and weight of immunodeficient nude mice. (C,D) circ-0000512, miR-622 and CMTM6 mRNA and protein expression in xenograft tumor tissues of immunodeficient nude mice as researched by qRT-PCR and Western blot respectively. (E) The image of xenograft tumor tissues in normal immune nude mice. (F) Xenograft tumor volume and weight of normal immune nude mice. (G,H) circ-0000512, miR-622, CMTM6 and PD-L1 mRNAs and proteins expression in xenograft tumor tissues of normal immune nude mice as explored by qRT-PCR and Western blot respectively. (I) CD8+ T cells in xenograft tumor tissues of normal immune nude mice as detected by IHC. ** $P < 0.01$ vs shNC group. IHC, immunohistochemistry; NC, negative control; qRT-PCR; quantitative reverse transcription PCR; TNBC, triple-negative breast cancer.

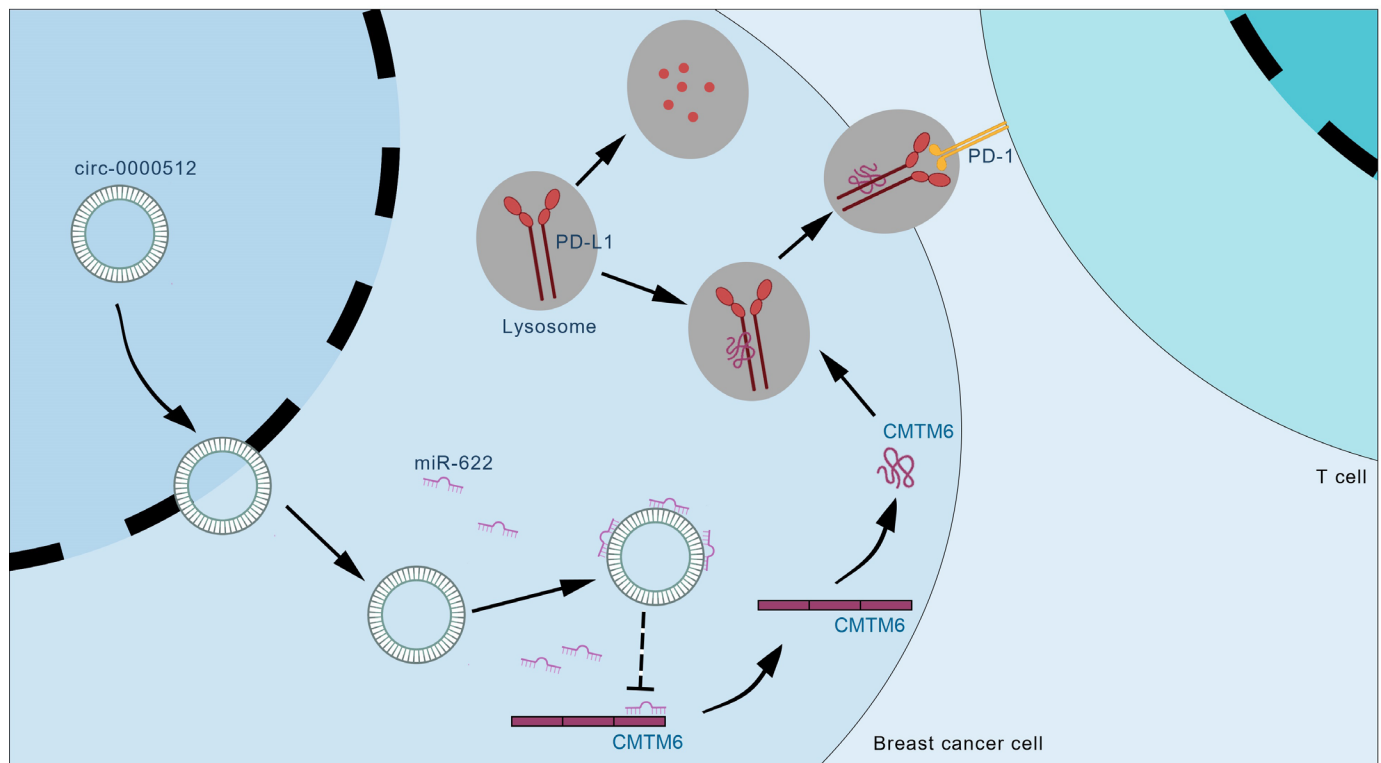


Figure 7 The molecular mechanism of circ-0000512/miR-622/CMTM6 axis in regulating TNBC progression. TNBC, triple-negative breast cancer.

induction of death during the immune escape process.³² CXCL10, CCL2, IL2, IFNG and STAT1 are the common immune activation genes, which can repress immune escape of tumor cells by enhancing the immune responsiveness, and facilitate T cells proliferation and expansion to tumor lesion site.^{33 34} Thus, circ-0000512 knockdown might suppress the immune escape of TNBC cells by inducing the expression of CXCL10, CCL2, IL2, IFNG and STAT1.

Intriguingly, this study found that circ-0000512 knockdown or overexpression did not significantly affect PD-L1 mRNA expression, but markedly reduced the PD-L1 protein expression in TNBC cells. Further research illustrated that circ-0000512 knockdown reduced the PD-L1 protein expression in TNBC cells by promoting its ubiquitination. The opposite results were found on circ-0000512 overexpression. PD-L1 is an immunosuppressive molecule expressed by tumor cells, which can facilitate tumor progression by suppressing the T cell-mediated immune response.²⁵ The post-translational modification of PD-L1 is a crucial mechanism of tumor immune suppression.²⁵ Ubiquitination is one of the main ways of PD-L1 post-translational modification, which effectively enhances the immunosuppression activity of PD-L1 and then attenuates the immune escape of tumor cells.³⁵ This study revealed that circ-0000512 knockdown might attenuate the immune escape of TNBC cells by promoting PD-L1 ubiquitination.

As previously reported, CMTM6 and CSN5 are two important genes in suppressing the ubiquitination of

PD-L1.²⁵ This study researched the effect of circ-0000512 on the expression of CMTM6 and CSN5. It was discovered that circ-0000512 knockdown reduced CMTM6 expression at both mRNA and protein levels, but did not significantly affect CSN5 expression at both mRNA and protein levels. In-depth research revealed that CMTM6 knockdown reduced PD-L1 expression at protein level by promoting its ubiquitination. CMTM6 is an important regulator of PD-L1 expression. Its knockdown can prominently reduce PD-L1 expression on the surface of TNBC cells, thereby attenuating TNBC aggressiveness and immune escape.³⁶ The high CMTM6 expression indicated unfavorable PFS of patients with TNBC.¹⁸ This study revealed that CMTM6 was highly expressed in patients with TNBC. CMTM6 knockdown reduced PD-L1 protein expression in TNBC cells by promoting its ubiquitination. Therefore, circ-0000512 knockdown might weaken TNBC progression and immune escape by promoting PD-L1 ubiquitination through reducing CMTM6 expression.

Further research was performed to verify the above speculation. It was demonstrated that circ-0000512 directly suppressed miR-622 expression, while miR-622 directly reduced CMTM6 expression at both mRNA and protein levels. Meanwhile, miR-622 was lowly expressed in patients with TNBC. Therefore, circ-0000512 might inhibit PD-L1 ubiquitination via sponging the miR-622/CMTM6 axis, thus promoting TNBC progression and immune escape. Previous study has detected the downregulated miR-622 expression in patients with BC, which is associated with unfavorable clinical outcomes.³⁷ miR-622

is also demonstrated as a tumor suppressor in some other human tumors, such as CRC, glioma, prostate cancer and renal cell carcinoma.^{38–41} As a result, these data indicated that circ-0000512 knockdown might weaken TNBC progression and immune escape by promoting PD-L1 ubiquitination through sponging the miR-622/CMTM6 axis.

CD8⁺ T cells play a crucial role in tumor immunity, which can induce the death of tumor cells. However, the lack of CD8⁺ T cells will result in immune evasion of tumor cells,⁴² while the immune escape of tumor cells to CD8⁺ T cells can induce tumor progression.²¹ Additionally, IFN γ and IL-2 can support the survival of tumor-reactive T cells and maintain the lethality of T cells against tumor cells.^{43,44} In this study, the activated CD8⁺ T cells were cocultured with TNBC cells. The results revealed that circ-0000512 knockdown increased the secretion of IFN γ and IL-2, as well as the proportions of CD8⁺ perforin⁺ T cells and CD8⁺ TNF- α ⁺ T cells, but reduced the OD value of TNBC cells. It should be noted that the levels of IFN γ and IL-2 were detected in the coculture medium after coculture of TNBC cells and CD8⁺ T cells. Therefore, it was difficult to verify the changes in IFN γ and IL2 secreted by CD8⁺ T cells in this coculture system. The changes in IFN γ and IL2 levels might be a result of a joint alteration of TNBC cells and CD8⁺ T cells. Nevertheless, one conclusion that could still be confirmed was that circ-0000512 knockdown enhanced the T cell killing ability.

More importantly, in vivo experiment indicated that circ-0000512 knockdown reduced tumor growth both in immunodeficient nude mice and normal immune mice. Simultaneously, circ-0000512 knockdown increased the CD8⁺ T cell proportion in xenograft tumors of normal immune mice. These in vivo data provided more solid theoretical foundation for the application of circ-0000512 as a therapeutic target for TNBC.

This paper had limitations. In this paper, circ-0000512 was proved to promote the expression of CMTM6, while CMTM6 could inhibit the ubiquitination and prolong the half-life of PD-L1 in TNBC cells. In order to visually validate that circ-0000512 could inhibit the ubiquitination and prolong the half-life of PD-L1 by promoting CMTM6 expression, it should be better to do experiments about the half-life and ubiquitination of PD-L1 after overexpressing CMTM6 in circ-0000512 knockdown cells. Furthermore, the expression and function of circ-0000512 in non-TNBC should be researched. These will be carried out in our future studies as current laboratory conditions do not allow us to perform these experiments.

Conclusion

In summary, this article was the first to investigate the function of circ-0000512 in TNBC progression. It was discovered that circ-0000512 was highly expressed in patients with TNBC and cells. circ-0000512 knockdown attenuated the progression and immune escape of TNBC both in vitro and in vivo. Meanwhile, circ-0000512 knockdown enhanced the lethality of CD8⁺ T cells against

TNBC cells. Typically, the mechanism might be that circ-0000512 inhibited PD-L1 ubiquitination by sponging the miR-622/CMTM6 axis, thus promoting TNBC progression and immune escape. Therefore, circ-0000512 might be an effective therapeutic target for TNBC.

Contributors L-FD, F-FC and H-HC designed the study. L-FD, H-HC and Y-FF performed the experiments. L-FD, F-FC, and KZ analyzed the data. All authors drafted the manuscript. All authors read the paper and approved the final manuscript. L-FD is responsible for the overall content as the guarantor.

Funding The authors have not declared a specific grant for this research from any funding agency in the public, commercial or not-for-profit sectors.

Competing interests None declared.

Patient consent for publication Consent obtained directly from patient(s)

Ethics approval This study was approved by the Ethics Committee of Women's Hospital, Zhejiang University School of Medicine (No. 20160056) and complied with the Declaration of Helsinki. All patients participated in this study voluntarily and signed the written informed consent.

Provenance and peer review Not commissioned; externally peer reviewed.

Data availability statement Data are available on reasonable request.

Supplemental material This content has been supplied by the author(s). It has not been vetted by BMJ Publishing Group Limited (BMJ) and may not have been peer-reviewed. Any opinions or recommendations discussed are solely those of the author(s) and are not endorsed by BMJ. BMJ disclaims all liability and responsibility arising from any reliance placed on the content. Where the content includes any translated material, BMJ does not warrant the accuracy and reliability of the translations (including but not limited to local regulations, clinical guidelines, terminology, drug names and drug dosages), and is not responsible for any error and/or omissions arising from translation and adaptation or otherwise.

Open access This is an open access article distributed in accordance with the Creative Commons Attribution Non Commercial (CC BY-NC 4.0) license, which permits others to distribute, remix, adapt, build upon this work non-commercially, and license their derivative works on different terms, provided the original work is properly cited, appropriate credit is given, any changes made indicated, and the use is non-commercial. See <http://creativecommons.org/licenses/by-nc/4.0/>.

ORCID iD

Li-Feng Dong <http://orcid.org/0000-0002-8478-7677>

REFERENCES

- Malhotra MK, Emens LA. The evolving management of metastatic triple negative breast cancer. *Semin Oncol* 2020;47:229–37.
- Borri F, Granaglia A. Pathology of triple negative breast cancer. *Semin Cancer Biol* 2021;72:136–45.
- Zajac O, Leclerc R, Nicolas A, et al. AXL controls directed migration of Mesenchymal triple-negative breast cancer cells. *Cells* 2020;9:247.
- Yin L, Duan J-J, Bian X-W, et al. Triple-negative breast cancer molecular Subtyping and treatment progress. *Breast Cancer Res* 2020;22:61.
- Sun X, Wang M, Wang M, et al. Metabolic Reprogramming in triple-negative breast cancer. *Front Oncol* 2020;10:428.
- da Silva JL, Cardoso Nunes NC, Izetti P, et al. Triple negative breast cancer: a thorough review of biomarkers. *Crit Rev Oncol Hematol* 2020;145:S1040-8428(19)30241-0.
- Li Z et al. Roles of circular RNA in breast cancer: present and future. *Am J Transl Res* 2019;11:3945–54.
- Jahani S, Nazeri E, Majidzadeh-A K, et al. Circular RNA; a new biomarker for breast cancer: A systematic review. *J Cell Physiol* 2020;235:5501–10. 10.1002/jcp.29558 Available: <https://onlinelibrary.wiley.com/doi/10.1002/jcp.29558>
- Zhou S, Chen W, Yang S, et al. The emerging role of circular RNAs in breast cancer. *Bioscience Reports* 2019;39.
- Jiang J, Lin H, Shi S, et al. Hsa_Circrna_0000518 facilitates breast cancer development via regulation of the miR-326/Fgfr1 axis. *Thorac Cancer* 2020;11:3181–92.
- Geng Y, Zheng X, Hu W, et al. Hsa_Circ_0009361 acts as the sponge of miR-582 to suppress colorectal cancer progression by regulating Apc2 expression. *Clinical Science* 2019;133:1197–213.

- 12 Wang L, Wu H, Chu F, *et al.* Knockdown of Circ_0000512 inhibits cell proliferation and promotes apoptosis in colorectal cancer by regulating miR-296-5p/Runx1 axis. *Oncol Targets Ther* 2020;13:7357–68.
- 13 Zhao G, Dai GJ. Hsa_Circrna_000166 promotes cell proliferation, migration and invasion by regulating miR-330-5p/Elk1 in colon cancer. *Oncol Targets Ther* 2020;13:5529–39.
- 14 Zhao X, Wang Y, Yu Q, *et al.* Circular Rnas in gastrointestinal cancer: Current knowledge, biomarkers and targeted therapy (review). *Int J Mol Med* 2020;46.
- 15 Zhang F, Li K, Pan M, *et al.* miR-589 promotes gastric cancer aggressiveness by a LIFR-Pi3K/AKT-C-Jun regulatory feedback loop. *J Exp Clin Cancer Res* 2018;37:152.
- 16 Santos JMO, Peixoto da Silva S, Gil da Costa RM, *et al.* The emerging role of Micrnas and other non-coding Rnas in cancer Cachexia. *Cancers (Basel)* 2020;12:1004.
- 17 Liu C, Min L, Kuang J, *et al.* Bioinformatic identification of miR-622 key target genes and experimental validation of the miR-622-Rnf8 axis in breast cancer. *Front Oncol* 2019;9:1114.
- 18 Tian Y, Sun X, Cheng G, *et al.* The Association of Cmtm6 expression with prognosis and PD-L1 expression in triple-negative breast cancer. *Ann Transl Med* 2021;9:131.
- 19 Qin T, Li B, Feng X, *et al.* Abnormally elevated Usp37 expression in breast cancer stem cells regulates Stemness, epithelial-Mesenchymal transition and cisplatin sensitivity. *J Exp Clin Cancer Res* 2018;37:287.
- 20 Gavilán E *et al.* Breast cancer cell line MCF7 escapes from G1/S arrest induced by Proteasome inhibition through a GSK-3B dependent mechanism. *Sci Rep* 2015;5:10027.
- 21 Zhang M, Wang N, Song P, *et al.* Lncrna Gata3-As1 facilitates tumour progression and immune escape in triple-negative breast cancer through Destabilization of Gata3 but stabilization of PD-L1. *Cell Prolif* 2020;53:53. 10.1111/cpr.12855 Available: <https://onlinelibrary.wiley.com/doi/10.1111/cpr.12855>
- 22 Ma Y, Xia P, Wang Z, *et al.* Pdia6 promotes Pancreatic cancer progression and immune escape through Csn5-mediated Deubiquitination of B-Catenin and PD-L1. *Neoplasia* 2021;23:912–28.
- 23 Cha J-H, Yang W-H, Xia W, *et al.* Metformin promotes antitumor immunity via Endoplasmic-Reticulum-associated degradation of PD-L1. *Mol Cell* 2018;71:606–20.
- 24 Burr ML, Sparbier CE, Chan Y-C, *et al.* Cmtm6 maintains the expression of PD-L1 and regulates anti-tumour immunity. *Nature* 2017;549:101–5.
- 25 Hsu J-M, Li C-W, Lai Y-J, *et al.* Posttranslational modifications of PD-L1 and their applications in cancer therapy. *Cancer Res* 2018;78:6349–53.
- 26 Zang Y, Li J, Wan B, *et al.* circRNA Circ-Ccnd1 promotes the proliferation of Laryngeal squamous cell carcinoma through elevating Ccnd1 expression via interacting with Hur and miR-646. *J Cell Mol Med* 2020;24:2423–33. 10.1111/jcmm.14925 Available: <https://onlinelibrary.wiley.com/doi/10.1111/jcmm.14925>
- 27 Değerli E, Torun V, Cansaran-Duman D. miR-185-5p response to Usnic acid suppresses proliferation and regulating apoptosis in breast cancer cell by targeting Bcl2. *Biol Res* 2020;53:19.
- 28 Zhao X. miR-1258 regulates cell proliferation and cell cycle to inhibit the progression of breast cancer by targeting E2F1. *Biomed Res Int* 2020;2020:1480819.
- 29 Jiang D, Song Y, Cao W, *et al.* P53-independent role of MYC mutant T58A in the proliferation and apoptosis of breast cancer cells. *Oncol Lett* 2019;17:1071–9.
- 30 Juríková M, Danihel Ľ, Polák Š, *et al.* Ki67, PCNA, and MCM proteins: markers of proliferation in the diagnosis of breast cancer. *Acta Histochem* 2016;118:544–52.
- 31 Hu C-C, Liang Y-W, Hu J-L, *et al.* Lncrna Rusc1-As1 promotes the proliferation of breast cancer cells by epigenetic silence of Klf2 and Cdkn1A. *Eur Rev Med Pharmacol Sci* 2019;23:6602–11.
- 32 Yin SS, Gao FH. Molecular mechanism of tumor cell immune escape mediated by Cd24/Siglec-10. *Front Immunol* 2020;11:1324.
- 33 Bendickova K, Fric J. Roles of IL-2 in bridging adaptive and innate immunity, and as a tool for cellular Immunotherapy. *J Leukoc Biol* 2020;108:427–37.
- 34 Yang L-S, Shi C-Y, Liang Y-H, *et al.* Bioinformatics analysis of programmed cell death ligand 1 Co-expression genes and their regulatory network in head and neck squamous cell carcinoma. *Hua Xi Kou Qiang Yi Xue Za Zhi* 2019;37:516–20.
- 35 Li C-W, Lim S-O, Xia W, *et al.* Glycosylation and stabilization of programmed death Ligand-1 suppresses T-cell activity. *Nat Commun* 2016;7:12632.
- 36 Xiao M, Hasmim M, Lequeux A, *et al.* Epithelial to Mesenchymal transition regulates surface PD-L1 via Cmtm6 and Cmtm7 induction in breast cancer. *Cancers* 2021;13:1165.
- 37 Orlandella FM, Mariniello RM, Mirabelli P, *et al.* miR-622 is a novel potential biomarker of breast carcinoma and impairs motility of breast cancer cells through targeting Nuak1 kinase. *Br J Cancer* 2020;123:426–37.
- 38 Fang Y, Sun B, Wang J, *et al.* miR-622 inhibits angiogenesis by suppressing the Cxcr4-VEGFA axis in colorectal cancer. *Gene* 2019;699:37–42.
- 39 Xu J, Ma B, Chen G, *et al.* MicroRNA-622 suppresses the proliferation of glioma cells by targeting Yap1. *J Cell Biochem* 2018;119:2492–500. 10.1002/jcb.26343 Available: <https://onlinelibrary.wiley.com/doi/10.1002/jcb.26343>
- 40 Targhazeh N, Yousefi B, Asghari S, *et al.* Mir-622 acts as a tumor suppressor to induce cell apoptosis and inhibit metastasis in human prostate cancer. *Andrologia* 2021;53:e14174. 10.1111/and.14174 Available: <https://onlinelibrary.wiley.com/doi/10.1111/and.14174>
- 41 Li T, Sun X, Xu K. The suppressing role of miR-622 in renal cell carcinoma progression by down-regulation of Ccl18/MAPK signal pathway. *Cell Biosci* 2018;8:17.
- 42 Fang W, Zhou T, Shi H, *et al.* Progranulin induces immune escape in breast cancer via up-regulating PD-L1 expression on tumor-associated Macrophages (Tams) and promoting Cd8(+) T cell exclusion. *J Exp Clin Cancer Res* 2021;40:4.
- 43 Kleborn LE, Berrien-Elliott MM, Yuan J, *et al.* Rescue of tolerant Cd8+ T cells during cancer Immunotherapy with IL2:antibody complexes. *Cancer Immunol Res* 2016;4:1016–26.
- 44 Canale FP, Ramello MC, Núñez N, *et al.* Cd39 expression defines cell exhaustion in tumor-infiltrating Cd8(+) T cells. *Cancer Res* 2018;78:115–28.